

Modeling the Impact of Back Contact Variation on $\text{CH}_3\text{NH}_3\text{SnI}_3$ - Based Perovskite Solar Cells Using SCAPS-1D

¹Nidhi Singh, ¹Anchal Srivastava, ²Susheel Kumar Singh, ³K. C. Dubey,

⁴Shobhit Shukla, ⁵Priyanka Srivastava and ¹R. K. Shukla*

¹Department of Physics, University of Lucknow, Lucknow-226007

²Department of Physics, Dr. S.M.N.R. University, Lucknow-226017

³Department of Physics, Shia P.G. College, Lucknow-226020

⁴Department of Information Technology, Dr. S.M.N.R. University, Lucknow-226017

⁵Department of Physics, Dr. R.M.L. Avadh University, Ayodhya-224001

Email: rajeshkumarshukla00@gmail.com

Abstract: Perovskite solar cells (PSCs) have emerged as promising candidates in the field of photovoltaics due to their high efficiency and low-cost fabrication potential. However, most high-performance PSCs are based on lead-containing materials, raising significant environmental and health concerns that hinder their commercialization. To overcome this limitation, researchers are actively exploring eco-friendly, lead-free alternatives. In this study, a lead-free perovskite solar cell using $\text{CH}_3\text{NH}_3\text{SnI}_3$ as the absorber layer is proposed. The device structure includes fluorine-doped tin oxide (FTO) as the transparent conducting oxide, ZnO nanorods (ZnO:NR) as the electron transport layer (ETL), and Spiro-OMeTAD as the hole transport layer (HTL). The SCAPS-1D simulation tool is employed to analyze and optimize the performance of the device. Key parameters such as absorber layer thickness, doping concentration, defect density, and the thicknesses of the ETL and HTL were systematically varied to identify optimal conditions. The simulation results reveal that under optimized conditions, the device achieves a power conversion efficiency (PCE) of 18.49 %, with an open-circuit voltage (V_{oc}) of 0.9248 V, a short-circuit current density (J_{sc}) of 29.57 mA/cm², and a fill factor (FF) of 67.61 %. These findings support the potential of lead-free PSCs for sustainable solar energy applications.

Keywords: Perovskite Solar Cell, SCAPS-1D, $\text{CH}_3\text{NH}_3\text{SnI}_3$, HTL, ETL, Absorbed Layer

INTRODUCTION

As the world rapidly advances, the demand for electricity continues to rise

significantly. However, our conventional energy sources, particularly fossil fuels, are limited and depleting. Additionally, fossil fuel-based power generation contributes heavily to environmental pollution by emitting greenhouse gases such as chlorofluorocarbons (CFCs), which are harmful to the atmosphere. In light of these challenges, renewable energy has emerged as a sustainable and eco-friendly alternative. Among the various renewable energy sources, solar energy stands out as one of the most promising, as the sun is an abundant and inexhaustible source of energy. Solar panel technology plays a vital role in harnessing solar energy for electricity production. Several types of solar cells have been developed to convert sunlight into electricity, including crystalline silicon solar cells, amorphous silicon photovoltaic cells, cadmium telluride (Cd-Te) cells, copper indium gallium selenide (CIGS) cells, multi-junction photovoltaic cells, tandem solar cells, and the rapidly advancing perovskite solar cells. Perovskite solar cells have gained significant attention due to their high power conversion efficiency, low production cost, and easy fabrication process. Currently, researchers around the world are focusing on improving the stability and efficiency of perovskite solar cells, making them a strong candidate for next-generation photovoltaic technologies.

METHODOLOGY

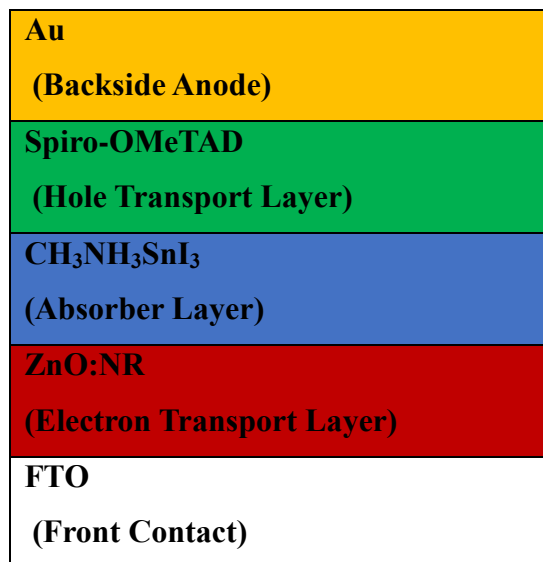
We employ numerical simulation using SCAPS-1D to enhance the efficiency of a lead-free planar heterostructure perovskite solar cell with an n-i-p configuration. The device features an intrinsic layer of methylammonium tin iodide ($\text{CH}_3\text{NH}_3\text{SnI}_3$), which functions as both the i-layer and absorber layer, while Spiro-OMeTAD serves as the hole transport layer (p-layer), and ZnO nanorods (ZnO:NR) act as the electron transport layer (n-layer). The primary objective of this simulation is to optimize the structural and material parameters of the device to improve its power conversion efficiency (PCE) and overall performance [1].

SCAPS-1D (Solar Cell Capacitance Simulator) is a widely used simulation tool that models the electrical and optical behaviour of thin-film solar cells. It supports a range of materials, including silicon, organic, and perovskite-based solar cells, making it highly adaptable for emerging photovoltaic technologies [2]. The simulation process in SCAPS involves defining

material properties, layer thicknesses, doping concentrations, and defect parameters, allowing researchers to investigate device behaviour under various operating conditions [3].

Numerical Modeling

The design follows a standard $\text{CH}_3\text{NH}_3\text{SnI}_3$ -based perovskite solar cell structure. As shown in Figure 1, the cell consists of an absorber layer, with an n-type ZnO:NR serving as the electron transport layer (ETL) at the bottom, and a p-type Spiro-OMeTAD layer functioning as the hole transport layer (HTL) at the top. This planar n-i-p configuration is commonly used to enhance charge separation and overall device efficiency [2].



Light Incident

Figure 1: Schematic representation of FTO/ $\text{ZnO:NR}/\text{CH}_3\text{NH}_3\text{SnI}_3/\text{Spiro-OMeTAD}/\text{Au}$ based solar cell.

The electrical properties considered in the simulation include thickness, band gap energy, electron affinity, electron and hole mobility, defect density, donor concentration, and acceptor concentration. These parameters can be modified to study their influence on device performance. Table 1 presents the detailed electrical parameters used in the SCAPS-1D simulation [4]. SCAPS-1D also enables the inclusion of interface layer properties, allowing

users to evaluate their impact on key performance metrics such as efficiency, open-circuit voltage, short-circuit current, and fill factor.

Table 1: Initial material parameters for proposed solar cell used in SCAPS Simulation

Physical Parameters	Symbol	Unit	FTO	Spiro-OMeTAD (HTL)	CH₃NH₃SnI₃	ZnO:NR (ETL)
Thickness	Th	nm	400	100	400	100
Energy Band Gap	E_g	eV	3.5	3.0	1.3	3.47
Electron Affinity	X	eV	4.0	2.45	4.17	4.3
Dielectric Permittivity (Relative)	ε_r	-	9.0	3.0	8.2	9.0
Density of States at Conduction Band	N_V	cm ⁻³	1×10 ¹⁸	2.2×10 ¹⁸	2.8×10 ¹⁸	2×10 ¹⁸
Density of States at Valence Band	N_C	cm ⁻³	1.8×10 ¹⁹	1.8×10 ¹⁹	3.9×10 ¹⁸	1.8×10 ²⁰
Thermal Velocity of Hole	V_e	cm/s	1×10 ⁷	1×10 ⁷	1×10 ⁷	1×10 ⁷
Thermal Velocity of electron	V_h	cm/s	1×10 ⁷	1×10 ⁷	1×10 ⁷	1×10 ⁷
Electron Mobility	μ_e	cm ² /V.s	20	2×10 ⁻⁴	0.16	100

Hole Mobility	μ_h	$\text{cm}^2/\text{V.s}$	10	2×10^{-4}	0.16	25
Uniform Shallow Donor Doping	N_D	cm^{-3}	1×10^{19}	0	-	1×10^{20}
Uniform Shallow Acceptor Doping	N_A	cm^{-3}	0	2×10^{18}	1×10^{15}	0
Defect Density	N_t	cm^{-3}	1×10^{15}	1×10^{15}	1×10^{15}	1×10^{15}
References			5	6	7	8

RESULT ANALYSIS

Optimization of the perovskite absorbing layer ($\text{CH}_3\text{NH}_3\text{SnI}_3$) thickness: The performance of a perovskite solar cell is highly dependent on the properties of the absorber layer, which plays a crucial role in light absorption and charge carrier generation. Previous studies have demonstrated that key photovoltaic parameters - including short-circuit current density (J_{sc}), open-circuit voltage (V_{oc}), fill factor (FF), and power conversion efficiency (PCE) - are influenced by the thickness of the absorber layer [9]. In this study, the absorber layer thickness was varied from 150 to 900 nm using SCAPS-1D simulation to investigate its impact on device performance. Figure 2 illustrates the trends observed in photovoltaic parameters as a function of absorber thickness. For the device structure FTO/ZnO:NR/ $\text{CH}_3\text{NH}_3\text{SnI}_3$ /Spiro-OMeTAD/Au, it was observed that as the thickness of the absorber layer increased, both V_{oc} and FF exhibited a declining trend. This suggests that excessive thickness may increase recombination losses and reduce carrier collection, thereby adversely affecting the overall efficiency of the solar cell.

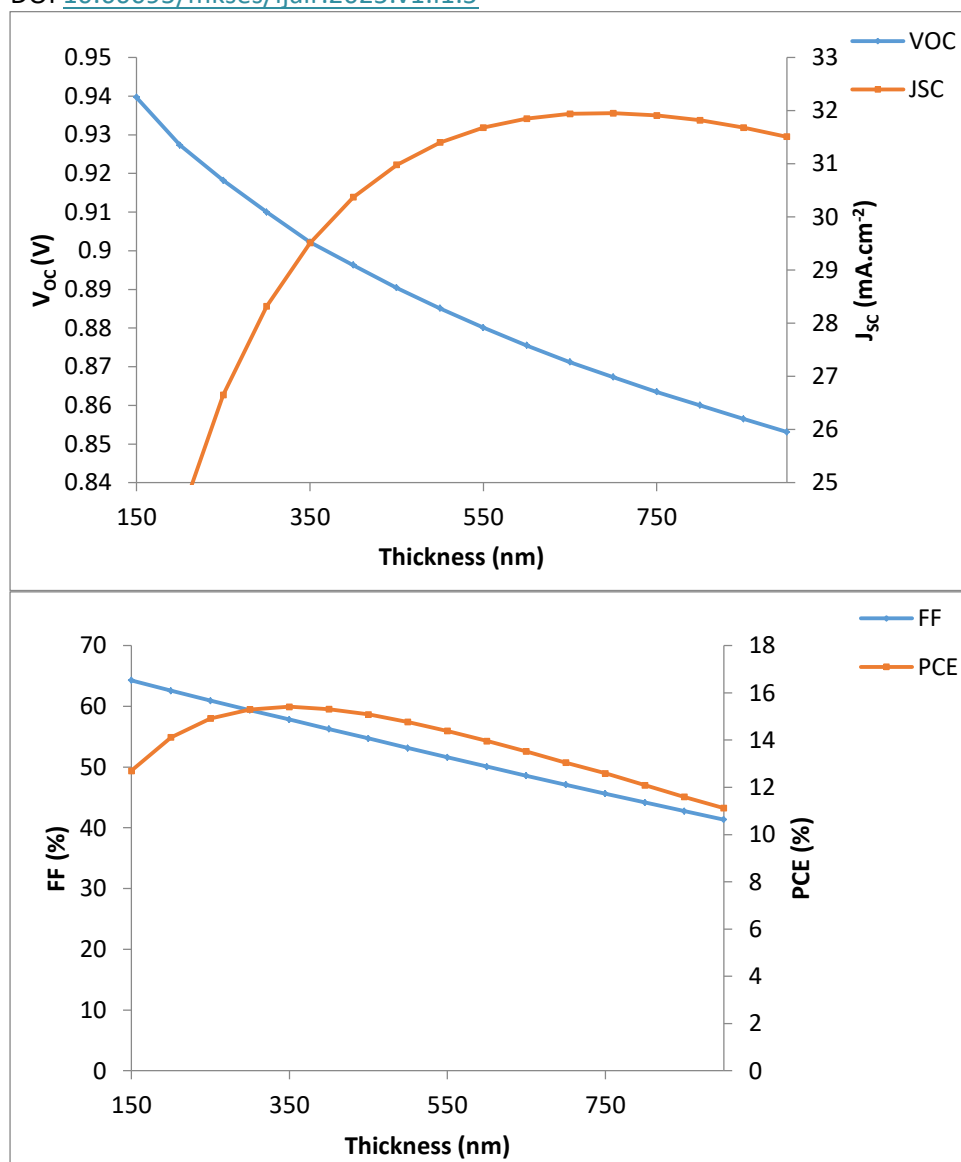


Figure 2: Variation of Solar Cell Parameters with thickness of absorber layer ($\text{CH}_3\text{NH}_3\text{SnI}_3$).

As the absorber layer thickness increases, the short-circuit current density (J_{sc}) also increases due to enhanced light absorption. However, the fill factor (FF) shows a decreasing trend, dropping from 64.28 % to 41.35 %. For the FTO/ZnO/ $\text{CH}_3\text{NH}_3\text{SnI}_3$ /Spiro-OMeTAD/Au configuration, the highest power conversion efficiency (PCE) of 15.41 % is achieved at an optimal absorber thickness of 350 nm, with $V_{oc} = 0.9028$ V, $J_{sc} = 29.51$ mA/cm², and FF = 57.84 %. The reduction in PCE at higher thicknesses is attributed to the limited diffusion length of charge carriers in the absorber layer, which increases recombination losses.

Optimization of donor density (N_D) of $\text{CH}_3\text{NH}_3\text{SnI}_3$ layer: The effect of uniform shallow donor doping concentration in the $\text{CH}_3\text{NH}_3\text{SnI}_3$ absorber layer was systematically explored to evaluate its influence on the performance of perovskite solar cells. Numerical simulations were performed using SCAPS-1D, with donor concentrations ranging from 10^{11} to 10^{16} cm^{-3} . Key photovoltaic parameters - including open-circuit voltage (V_{oc}), short-circuit current density (J_{sc}), fill factor (FF), and power conversion efficiency (PCE) - were examined to assess the impact of doping. As shown in Figure 3, donor concentration plays a crucial role in determining device performance. The highest PCE of approximately 15.60 % was observed at a donor concentration of $1 \times 10^{11} \text{ cm}^{-3}$, marking this as the optimal doping level. Beyond this point, increasing donor density caused a noticeable decline in V_{oc} , dropping from 0.9040 V to 0.8505 V. A slight reduction in J_{sc} was also observed, decreasing from 29.54 to 28.56 mA/cm². The fill factor declined from 58.43 to 56.69 %, possibly due to increased charge carrier recombination and changes in internal electric field distribution. These results highlight the importance of optimizing donor concentration in the absorber layer to achieve maximum efficiency in lead-free perovskite solar cells.

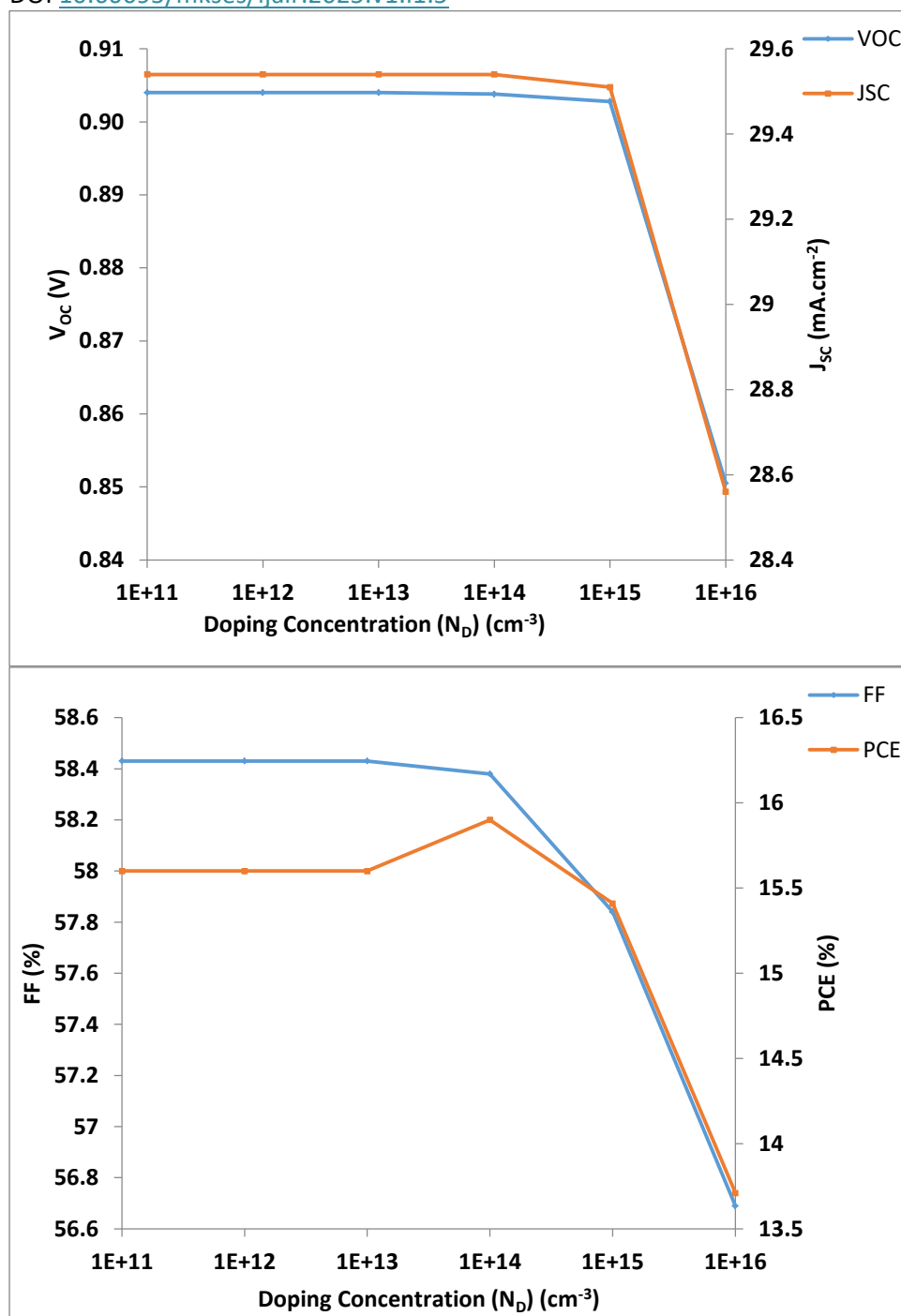


Figure 3: Effect of the donor density (N_D) of $\text{CH}_3\text{NH}_3\text{SnI}_3$ layer on Simulated parameters of solar cell.

Optimization of the absorber layer's ($\text{CH}_3\text{NH}_3\text{SnI}_3$) acceptor density (N_A): The doping concentration in the absorber layer significantly influences the photovoltaic performance of perovskite solar cells (PSCs). This numerical analysis investigates the effect of varying absorber doping concentrations on device performance. Figure 4 illustrates how the key photovoltaic parameters - open-circuit voltage (V_{oc}), short-circuit current density (J_{sc}), fill

factor (FF), and power conversion efficiency (PCE) - change with doping levels in the absorber layer. The doping concentration was varied from 1×10^{11} to 1×10^{17} cm^{-3} . Results show that V_{oc} , J_{sc} , and FF remain nearly constant up to 1×10^{13} cm^{-3} , after which all three parameters begin to improve. The PCE increases steadily and reaches its maximum at a doping level of 1×10^{16} cm^{-3} . Beyond this point, further increases in doping concentration lead to a decline in efficiency. This decrease is attributed to the formation of additional defect states or trap sites, which facilitate recombination losses [10]. The optimal doping concentration for the absorber layer for this configurations is found to be 1×10^{16} cm^{-3} , yielding $V_{oc} = 0.9239$ V, $J_{sc} = 29.48$ mA/cm^2 , FF = 59.32 %, and a maximum PCE of 16.16 %. These findings underscore the importance of carefully tuning absorber doping levels for optimal solar cell performance.

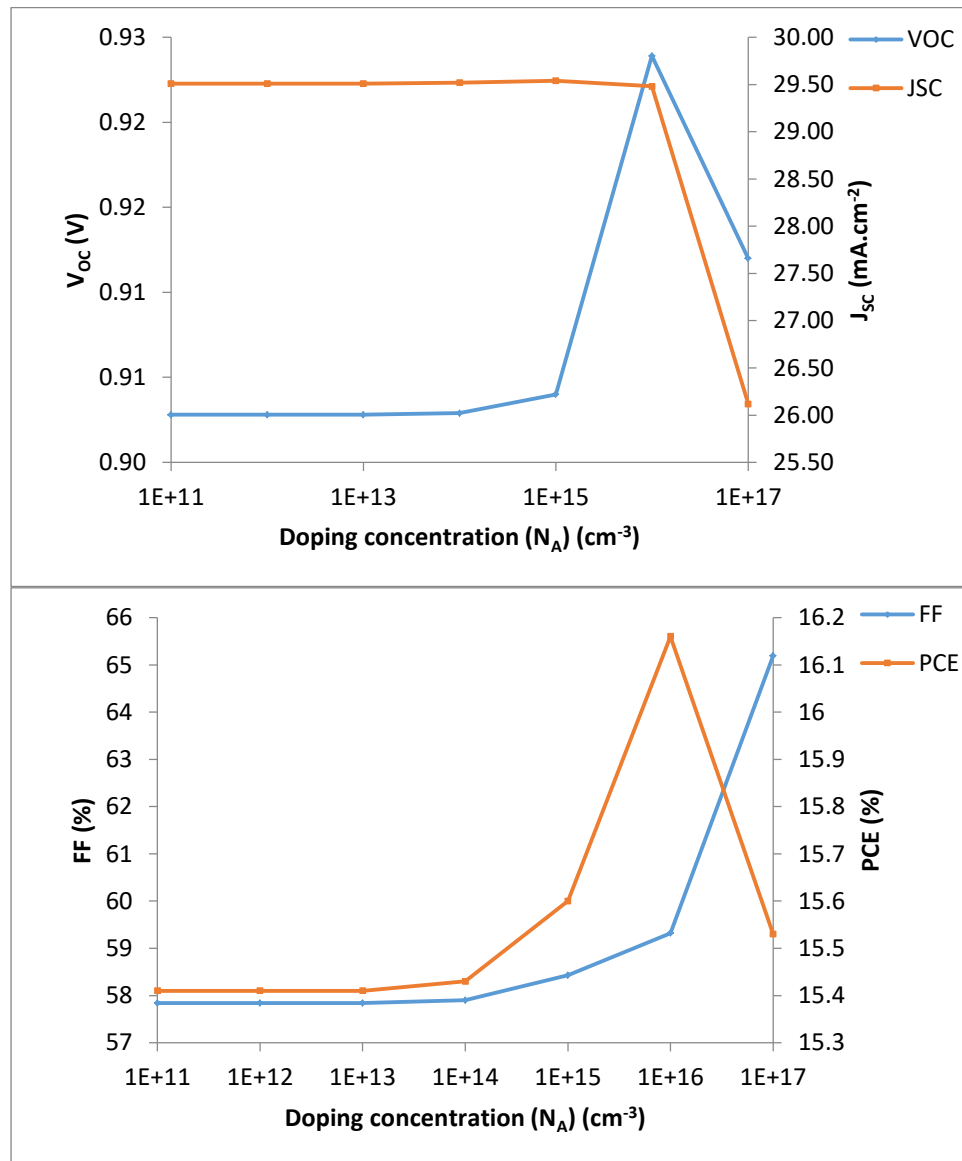


Figure 4: Variation of Solar Cell Parameters with shallow uniform acceptor density**(N_A) in absorption Layer (CH₃NH₃SnI₃).**

Optimization of absorber layer (CH₃NH₃SnI₃) defect density (N_t): Figure 5 illustrates the variation of photovoltaic parameters with respect to the defect density (cm⁻³) in the absorber layer. Understanding the impact of defect density is essential for optimizing device efficiency, as defects within the absorber act as recombination centers that reduce charge carrier lifetimes. The primary cause of defects stems from poor doping quality and improper doping techniques during absorber layer fabrication. Since the perovskite layer contains various defect energy levels, the Gaussian distribution effectively models these defect densities [11]. The simulation results show that the maximum power conversion efficiency (PCE) occurs at a defect density of 10¹⁵ cm⁻³, where the open-circuit voltage (V_{oc}) is 0.9239 V, short-circuit current density (J_{sc}) is 29.48 mA/cm², fill factor (FF) is 59.32 %, and PCE reaches 16.16 %. Beyond this optimal defect density, all key performance parameters - V_{oc}, J_{sc}, FF, and PCE - decline sharply, as shown in Figure 5. This decline is attributed to increased charge recombination and reduced carrier transport efficiency. Hence, controlling and minimizing defect density in the absorber layer is critical for achieving high-efficiency perovskite solar cells.

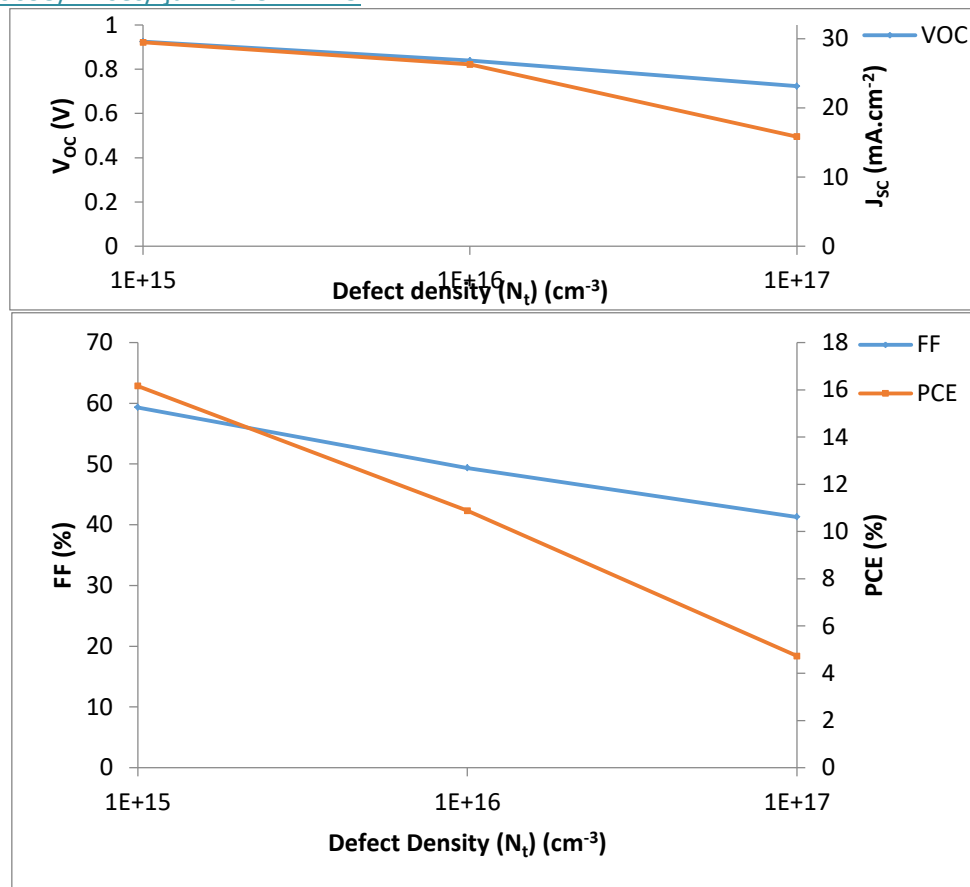


Figure 5: Changes in Solar Cell Specifications with Defect Density (N_t) (cm^{-3}) of absorber layer ($\text{CH}_3\text{NH}_3\text{SnI}_3$).

Optimization of the ETL (ZnO:NR) Thickness Variation: The thickness of the Electron Transport Layer (ETL), specifically ZnO nanorods (ZnO:NR), plays a critical role in the performance of $\text{CH}_3\text{NH}_3\text{SnI}_3$ -based perovskite solar cells. Variations in ETL thickness can significantly influence device efficiency by affecting charge transport and collection. In this study, the ETL thickness was systematically varied between 50 nm and 400 nm to determine the optimal value [12]. Results show that the ETL thickness strongly impacts the power conversion efficiency (PCE) and short-circuit current density (J_{sc}), while open-circuit voltage (V_{oc}) and fill factor (FF) remain largely unaffected. As the ETL thickness increases, both J_{sc} and PCE rise, reaching a saturation point around 100 nm. Beyond this thickness, further increases do not lead to significant improvements, indicating an optimal thickness range. Based on these observations, the ETL thickness was optimized to 100 nm, balancing efficient charge transport and light absorption, as illustrated in Figure 6. This optimization is crucial for enhancing the overall performance of perovskite solar cells.

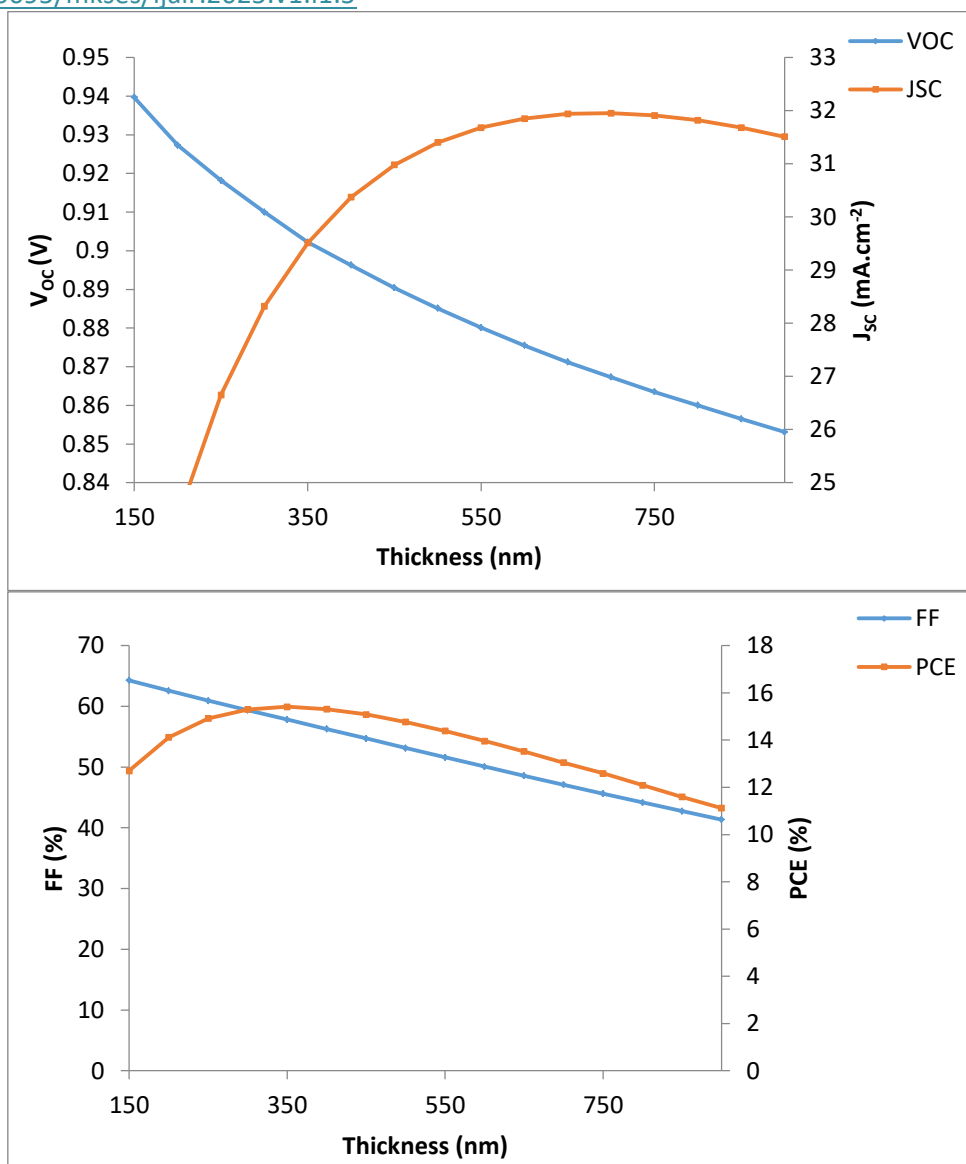


Figure 6: Changes in solar cell parameters according to ETL (ZnO:NR) thickness

Optimization of donor doping concentration (N_D) of ETL (ZnO:NR): To assess the impact of doping concentration on perovskite solar cell (PSC) performance, the donor impurity concentration (N_D) was varied from 10^{11} to 10^{20} cm⁻³. As shown in Figure 7, the power conversion efficiency (PCE) increases steadily from 1.71 to 16.16 % with rising N_D . This improvement is mainly due to reduced series resistance and enhanced optical conductivity in the electron transport material (ETM), which facilitates more efficient charge transport. The optimal doping concentration of 10^{20} cm⁻³ achieves a PCE of 16.16 %, with a short-circuit current density (J_{sc}) of 29.48 mA/cm², open-circuit voltage (V_{oc}) of 0.9239 V, and a fill factor (FF) of 59.32 %. At lower doping levels, reduced Auger recombination and minimized quenching losses contribute to better performance. These results highlight the

importance of carefully optimizing doping concentration to maximize efficiency while limiting recombination losses in perovskite solar cells.

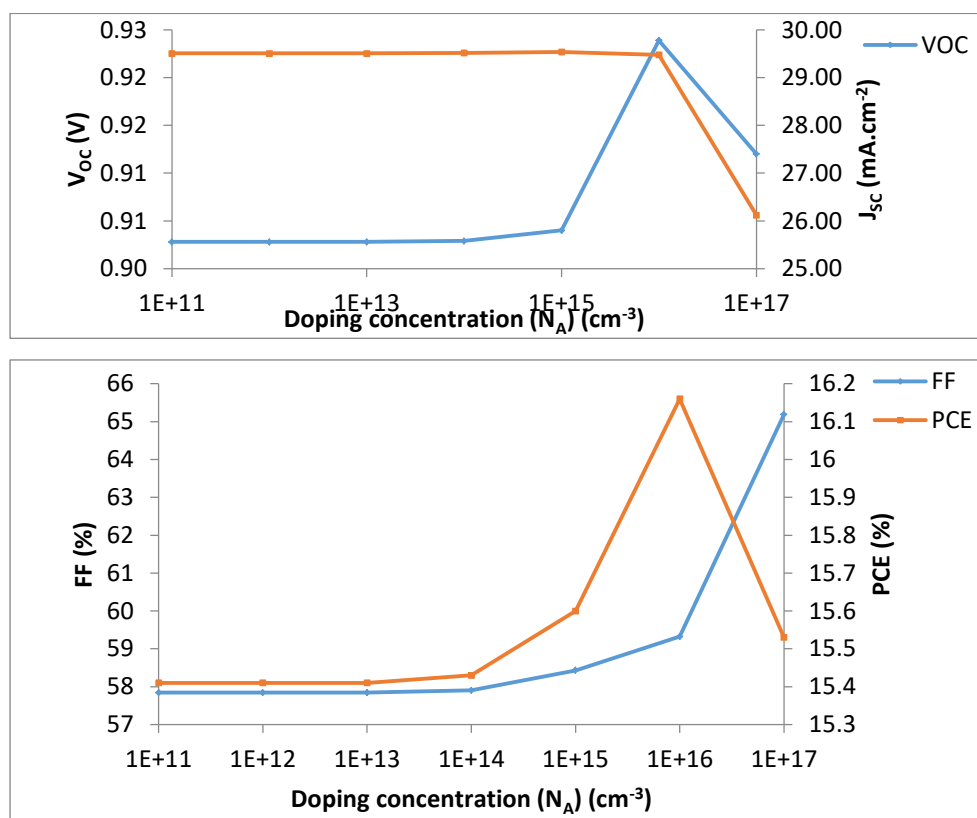


Figure 7: Variation of doping concentration of ETL (ZnO:NR) on the simulated parameters of solar cell.

Optimization of the Thickness variation HTL (Spiro-OMeTAD): The performance of a $\text{CH}_3\text{NH}_3\text{SnI}_3$ perovskite solar cell is significantly influenced by the thickness of its Hole Transport Layer (HTL) (Spiro-OMeTAD). In this study, the HTL thickness was varied between 25 nm and 400 nm to evaluate its effect on device efficiency. The open-circuit voltage (V_{oc}) and short-circuit current density (J_{sc}) remain nearly constant as the HTL thickness increases. However, both the fill factor (FF) and power conversion efficiency (PCE) show a slight decrease with increasing HTL thickness. The fill factor drops from 59.60 to 58.21 %, while the PCE decreases from 16.23 to 15.85 %, as illustrated in Figure 8. These results indicate that while V_{oc} and J_{sc} are stable, optimizing HTL thickness is important to maintain high FF and PCE for better overall solar cell performance.

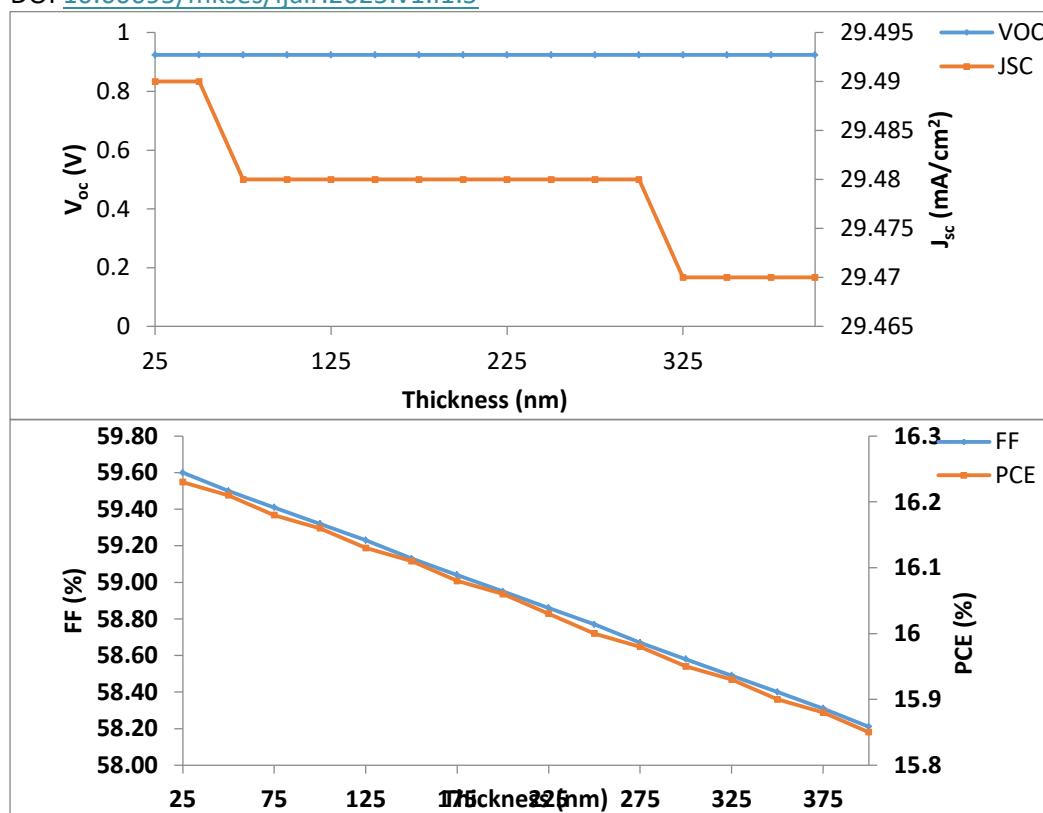


Figure 8: Changes in Solar Cell Parameters according to HTL (Spiro-OMeTAD) thickness.

For a variety of reasons, the solar cells' efficiency may not necessarily be greatly affected by the HTL thickness. With little recombination, HTL is intended to effectively transfer holes

Optimization of doping concentration (N_A) of HTL (Spiro-OMeTAD): The effect of acceptor impurity concentration (N_A) on perovskite solar cell (PSC) performance was examined over a range from 10^{11} to 10^{21} cm⁻³. Figure 9 demonstrates that N_A significantly influences the overall efficiency. The optimal performance was achieved at an acceptor concentration of 10^{21} cm⁻³, yielding a power conversion efficiency (PCE) of 18.49 %, short-circuit current density (J_{sc}) of 29.57 mA/cm², open-circuit voltage (V_{oc}) of 0.9248 V, and fill factor (FF) of 67.61 %. This concentration was selected for further analysis due to its stable and superior device performance.

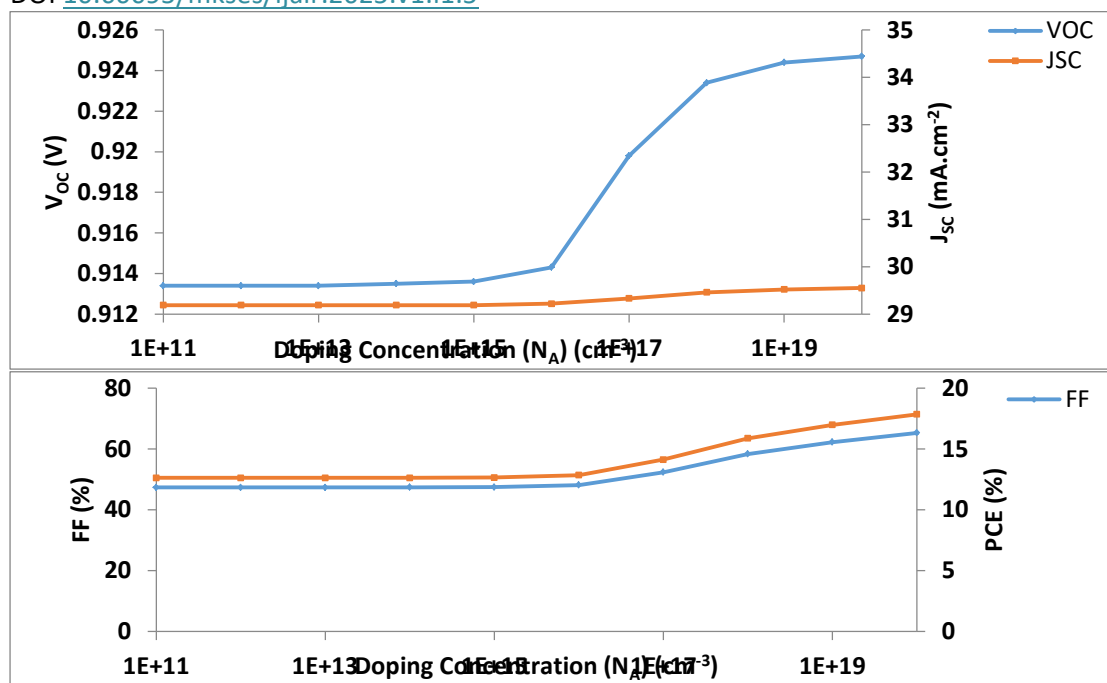


Figure 9: Variation of the simulated parameters with the doping concentration of HTL (Spiro-OMeTAD).

Effect of temperature: Understanding the impact of temperature on solar cell performance is essential for evaluating device stability and efficiency. In this study, temperatures ranging from 260 to 600 K were analyzed, revealing a significant decrease in power conversion efficiency (PCE) from 18.49 % at 300 K to 6.98 % at 600 K, as shown in Figure 10. This decline is primarily due to shorter charge carrier diffusion lengths, thermal stress-induced defects, and increased recombination rates, all of which negatively affect device performance. The open-circuit voltage (V_{oc}) decreases markedly from 0.9248 to 0.4230 V, while the short-circuit current density (J_{sc}) experiences a slight drop from 29.57 to 29.45 mA/cm^2 . The fill factor (FF) also declines significantly, falling from 67.61 to 56.06 %. These results highlight the challenges of maintaining high efficiency at elevated temperatures and emphasize the importance of incorporating effective thermal management strategies in the design and development of perovskite solar cells to ensure long-term stability and optimal performance.

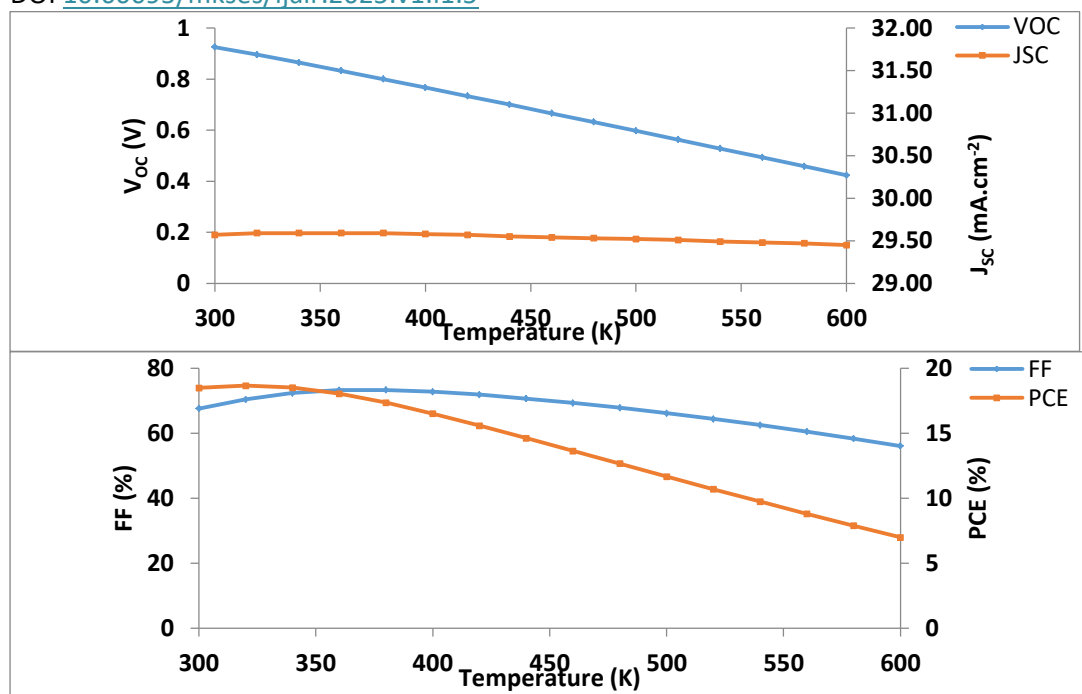


Figure 10: Variation of the simulated parameters with the temperature.

Effect of series resistance: In perovskite solar cells (PSCs), series resistance (R_s) originates from several factors, including the material layers, interface barriers, charge-collecting interlayers, and metal contacts. Shunt resistance, in contrast, is caused by leakage paths such as recombination losses and pinholes within the active layer. An increase in R_s restricts current flow, leading to a decline in power conversion efficiency (PCE), while the short-circuit current density (J_{sc}) and open-circuit voltage (V_{oc}) remain relatively stable. To understand R_s 's impact, it was varied between 0 and $10 \Omega \cdot \text{cm}^2$ in simulations. As shown in Figure 11, the PCE drops significantly from 18.49 % to 12.11 % with increasing R_s , accompanied by a notable decrease in the fill factor (FF). These results highlight the critical role of minimizing series resistance to achieve optimal device performance. Reducing R_s is essential for improving charge transport and overall efficiency, making it a key focus in the design and fabrication of high-performance PSCs.

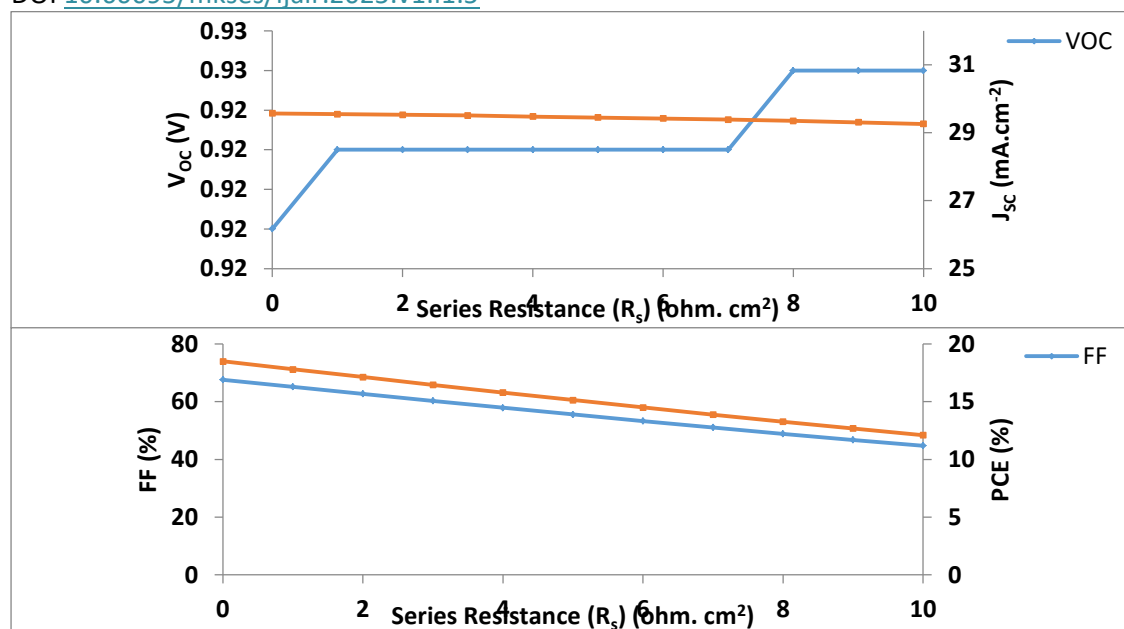


Figure 11: Effect of the simulated parameters with the series resistance.

Effect of shunt resistance: Figure 12 illustrates the impact of varying shunt resistance (R_{sh}) from 10^1 to $10^{10} \Omega \cdot \text{cm}^2$ on the performance of perovskite solar cells. As R_{sh} increases from 10^1 to $10^5 \Omega \cdot \text{cm}^2$, there is a significant improvement in open-circuit voltage (V_{oc}), power conversion efficiency (PCE), and fill factor (FF). Beyond $10^5 \Omega \cdot \text{cm}^2$, these parameters stabilize, while the short-circuit current density (J_{sc}) remains nearly constant throughout the range. The primary driver of the efficiency enhancement is the increase in fill factor. The optimal shunt resistance value for maximizing device performance is identified as $10^5 \Omega \cdot \text{cm}^2$. This level effectively minimizes leakage currents and recombination losses, thereby enabling peak efficiency in the proposed perovskite solar cells.

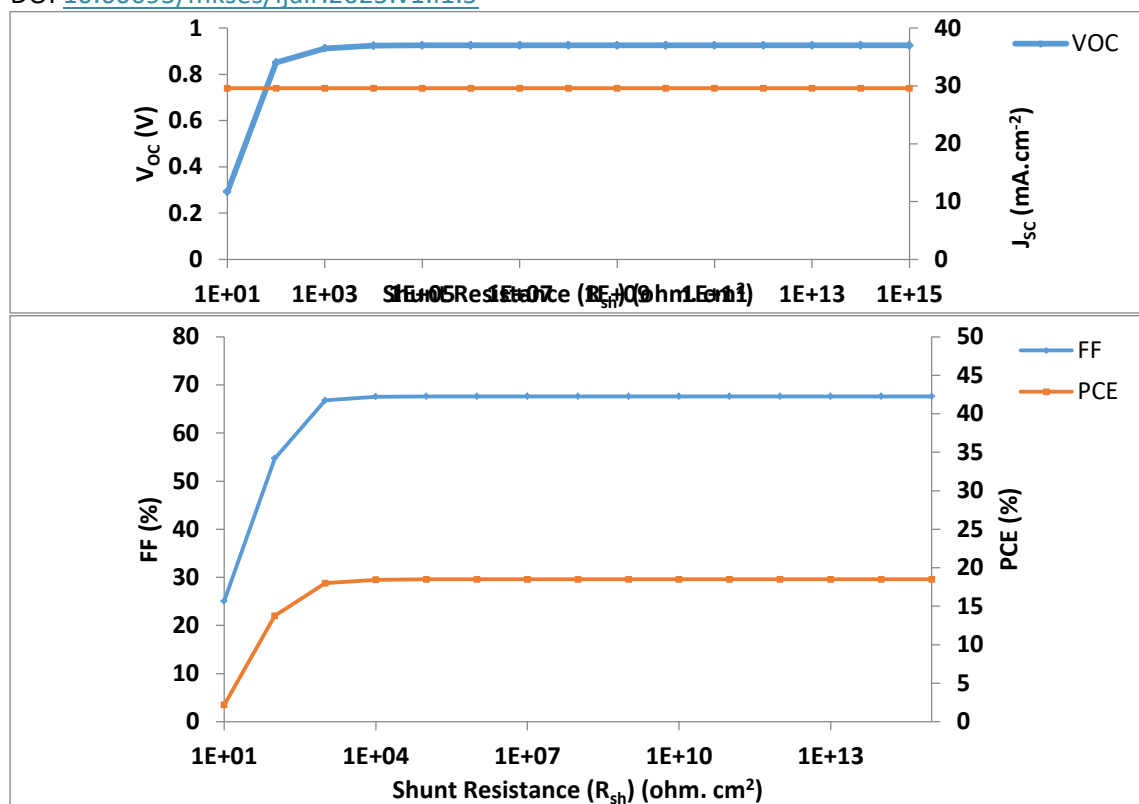


Figure 12: Effect of the simulated parameters with the shunt resistance.

Effect of back contact: The back metal contact plays a crucial role in the performance of perovskite solar cells by facilitating efficient charge extraction and influencing overall device efficiency. Figure 13 demonstrates the impact of varying the electron work function of the back contact metal from 4.8 to 5.6 eV on solar cell performance. As the work function increases from 4.8 to 5.3 eV, the open-circuit voltage (V_{oc}), fill factor (FF), and power conversion efficiency (PCE) all increase nearly linearly. Beyond 5.3 eV, these parameters plateau and remain stable up to 5.6 eV. Simulation results highlight nickel, with a work function of approximately 5.3 eV, as a promising and cost-effective alternative to gold for the back contact. Using nickel can enhance device performance by maximizing V_{oc} and PCE, while potentially reducing manufacturing costs. This finding underscores the importance of carefully selecting back contact materials to optimize both efficiency and long-term stability in perovskite solar cell design.

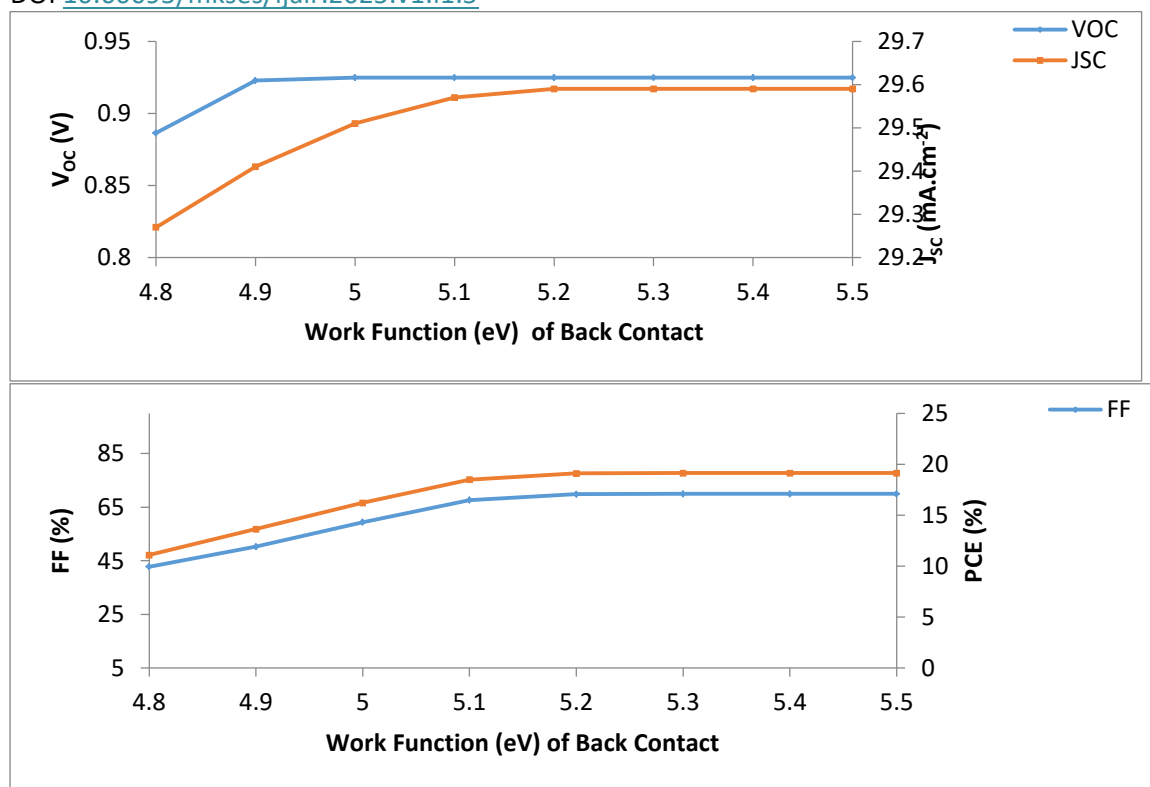


Figure 13: output parameters (V_{oc} , J_{sc} , FF, PCE) as a function of electron work function of back metal contact of the proposed solar cell structure.

Optimized device: Table 2 presents the optimized solar cell parameters, while Figure 14 illustrates the schematic of the optimized device alongside its current-voltage (J-V) characteristics. The optimized solar cell achieves a power conversion efficiency (PCE) of 18.49 %, a fill factor (FF) of 67.61 %, a short-circuit current density (J_{sc}) of 29.57 mA/cm², and an open-circuit voltage (V_{oc}) of 0.9248 V. Table 3 compares these results with the initial device parameters, highlighting notable improvements in performance due to the optimization process.

Table 2: The optimized parameters of the device.

Physical Parameters	Symbol	Unit	Spiro-OMeTAD (HTL)	MASnI_3	ZnO:NR (ETL)
Thickness	Th	Nm	25	350	100
Uniform Shallow Donor	N_D	cm^{-3}	-	1×10^{11}	1×10^{20}

Doping					
Uniform Shallow Acceptor Doping	N_A	cm^{-3}	1×10^{21}	1×10^{16}	-
Defect Density	N_t	cm^{-3}	1×10^{11}	1×10^{15}	1×10^{11}

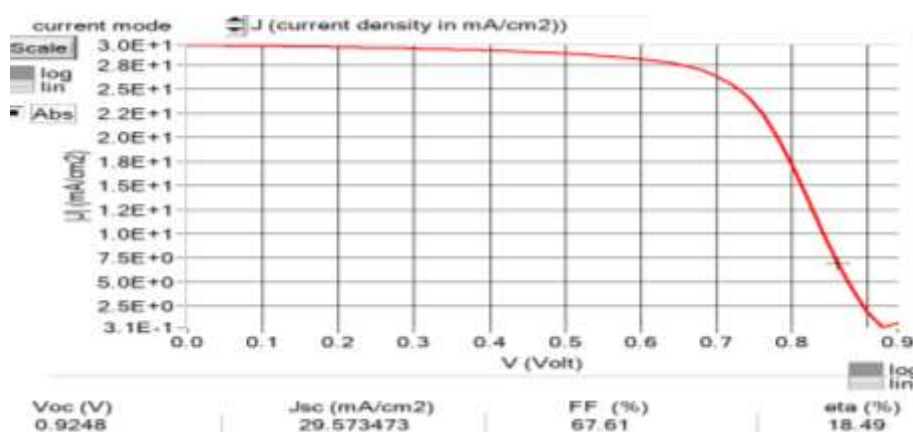


Figure 14: Optimized device: J-V curve.

Table 3: Output parameters of the optimized device and those of the initial one.

Output parameters	FF (%)	J_{sc} (mA/cm ²)	V_{oc} (V)	PCE (%)
Initial device	56.26	30.37	0.8963	15.91
Optimized device	67.61	29.57	0.9248	18.49

Conclusion: Using SCAPS-1D software, a Sn-based perovskite solar cell was designed and simulated in this study. The simulation focused on optimizing a device structure with $\text{CH}_3\text{NH}_3\text{SnI}_3$ as the absorber layer. By systematically investigating key factors such as layer thickness, doping concentrations, and defect densities, the study identified conditions that enhance solar cell performance. The optimized device achieved a power conversion efficiency (PCE) of 18.49 %, a short-circuit current density (J_{sc}) of 29.57 mA/cm², an open-circuit voltage (V_{oc}) of 0.9248 V, and a fill factor (FF) of 67.61 %. These results highlight $\text{CH}_3\text{NH}_3\text{SnI}_3$'s strong potential as an effective and environmentally friendly absorber material for perovskite photovoltaics. The findings offer valuable insights into how material properties

and device parameters influence solar cell efficiency. This research lays the groundwork for experimental validation and the future development of scalable, high-efficiency, lead-free perovskite solar cells, indicating promising prospects for commercial manufacturing of this Sn-based PSC technology.

Funding statement: This research did not obtain financial support from any specific grant provided by funding agencies in the public, commercial, or not-for-profit sectors.

Data availability statement: Data will be made available on request.

Declaration of interest's statement: The authors declare no conflict of interest.

Additional information: No additional information is available for this paper.

Acknowledgements: We would like to express our gratitude to Dr. Marc Burgelman and their team from Ghent University, Belgium, for providing access to the SCAPS simulator, which has been instrumental in conducting the simulations for this research.

Institutional Review Board Statement: Not applicable.

Informed Consent Statement: Not applicable.

REFERENCES

1. M. Burgelman, P. Nollet, S. Degrave, Modelling Polycrystalline Semiconductor Solar Cells, *Thin Solid Films*, 361 (2000) 527-532.
2. M. Burgelman, K. Decock, S. Khelifi And A. Abass, Advanced Electrical Stimulation of Thin Film Solar Cells, *Thin Solid Films*, 535 (2013) 296-301.
3. Kanoun, A.-A.; Kanoun, M.B.; Merad, A.E.; Goumri-Said, S. Toward Development Of High-Performance Perovskite Solar Cells Based On $\text{CH}_3\text{NH}_3\text{GeI}_3$ Using Computational Approach. *Sol. Energy* 2019, 182, 237–244.
4. Hao, L.; Zhou, M.; Song, Y.; Ma, X.; Wu, J.; Zhu, Q.; Fu, Z.; Liu, Y.; Hou, G.; Li, T. Tin-Based Perovskite Solar Cells: Further Improve The Performance of The Electron Transport Layer-Free Structure By Device Simulation. *Sol. Energy* 2021, 230, 345–354.
5. Fozia Arif, Muhammad Aamir, Ahmed Shuja, Md. Shahiduzzaman, Javeed Akhtar, Simulation and numerical modeling of high performance $\text{CH}_3\text{NH}_3\text{SnI}_3$ solar cell with cadmium sulfide as electron transport layer by SCAPS-1D, *Results in Optics*, Volume 14, 2024, 100595,



[https://doi.org/10.1016/j.rio.2023.100595.](https://doi.org/10.1016/j.rio.2023.100595)

6. Bouazizi S, Tlili W, Bouich A, Soucase BM, Omri A. Design and efficiency enhancement of FTO/PC60BM/CsSn_{0.5}Ge_{0.5}I₃/Spiro-OMeTAD/Au perovskite solar cell utilizing SCAPS-1D Simulator, Materials Research Express. 2022 Sep 6;9(9):096402.
7. Sunny A, Rahman S, Khatun M, Ahmed SR. Numerical study of high performance HTL-free CH₃NH₃SnI₃-based perovskite solar cell by SCAPS-1D. AIP Advances. 2021 Jun 1;11(6).
8. Daoudi O, Jellal I, Haddout A, Benaicha I, Nouneh K, Idiri M, Lharch M, Fahoume M. The outcomes of Zn doping on the properties of CuO thin films prepared via modified SILAR method and its impact on the performance of CuO-based solar cells using Cd_{0.4}Zn_{0.6}S-ETL and Spiro-OMeTAD-HTL. Journal of Materials Science: Materials in Electronics. 2024 Jul;35(19):1353.
9. Shamna, M.S., Nithya, K.S. And Sudheer, K.S. (2020), Simulation and Optimization of CH₃NH₃SnI₃ Based Inverted Perovskite Solar Cell With NiO As Hole Transport Material, Materials Today: Proceedings, 33, Pp. 1246–1251. [https://doi.org/10.1016/J.Matpr.2020.03.488.](https://doi.org/10.1016/J.Matpr.2020.03.488)
10. M. Burgelman, J. Marlein, Analysis of Graded Band Gap Solar Cells With SCAPS, Proceedings of The 23rd European Photovoltaic Solar Energy Conference, Valencia, 2008, Pp. 2151-2155.
11. Mcghehee And T. Buonassisi, A 2-Terminal Perovskite/Silicon Multi-Junction Solar Cell Enable by a Silicon Tunnel Junction," Applied Physics Letters, Vol. 106, No. 12, 2015.
12. Fatema, K. And Arefin, M.S. (2022) Enhancing The Efficiency of Pb-Based And Sn-Based Perovskite Solar Cell By Applying Different ETL and HTL Using SCAPS-ID, Optical Materials, 125, P. 112036. Doi:10.1016/J.Optmat.2022.112036.